Highly porous macro- and micro-cellular ceramics from a polysilazane precursor

C. Vakifahmetoglu [a], I. Menapace [b], A. Hirsch [b], L. Biasetto [a,c],
R. Hauser [d], R. Riedel [b], P. Colombo [a,e,*]

[a] Università di Padova, Dipartimento di Ingegneria Meccanica, Via Marzolo 9, 35131 Padova, Italy
[b] Technische Universität Darmstadt, Petersenstr. 23, 64287 Darmstadt, Germany
[c] Istituto Nazionale di Fisica Nucleare, Laboratori Nazionali di Legnaro, V.le dell'Università 2, 35020 Legnaro, Padova, Italy
[d] Fraunhofer Institute for Manufacturing and Advanced Materials, Winterbergstr. 28, 01277 Dresden, Germany
[e] Department of Materials Science and Engineering, The Pennsylvania State University, University Park, PA 16802, USA

Abstract

Micro- and macro-cellular SiCN and SiOCN foams were produced via two different routes by using a polysilazane preceramic polymer. In the first route, a mixture of partially cross-linked polysilazane and poly(methylmetacrylate) microspheres, used as sacrificial fillers, was warm pressed and subsequently pyrolyzed to create micro-cellular foams. In the second route, liquid polysilazane was mixed with a physical blowing agent and the blend was cured and pyrolyzed, leading to the formation of macro-cellular ceramics in a one-step process. Ceramic components of different morphology and characteristics, depending on the processing method adopted, were fabricated. The foams had a mostly interconnected porosity ranging from ~60 to 80 vol% and possessing a compressive strength in the range ~1–11 MPa. Some oxygen contamination was found in the foams obtained using the sacrificial fillers, probably because of the adsorbed humidity on their surface. The polymer derived ceramic (PDC) route is an efficient and cost effective way to produce SiCN-based foams possessing tailored pore architecture and properties suitable for high temperature applications.
© 2009 Elsevier Ltd and Techna Group S.r.l. All rights reserved.

Keywords: Silicon carbonitride; Foams; Polysilazane preceramic polymer; Compression strength

1. Introduction

Ceramic foams are a specific group of cellular materials possessing a very favorable combination of properties, such as low density, low thermal conductivity and low dielectric constant, high permeability, high thermal shock resistance, high chemical stability and high specific strength [1,2]. As a result, these materials are used in different engineering applications ranging from metallurgy (removal of impurities from liquid metals) or high-temperature processing (thermal insulation) to the automotive (control of gas and diesel emissions), petrochemical (catalyst support), combustion technology (porous-medium burners), or biomedical (biological implants) fields [3–7]. The properties of cellular materials are affected by their relative density (amount of porosity), morphological characteristics (cell size and shape), distribution of the pores (pore interconnectivity and cell wall/strut porosity), and finally the material type [8].

It has been recently demonstrated that preceramic polymers can be used to produce highly porous structures (foams, membranes, components with hierarchical porosity) of various compositions (SiC, Si_3N_4, SiOC, SiOCN, SiCN and Si(E)CN (E = B, Al, Ti, etc.)) and morphologies [3,5,9]. In particular, poly-siloxane and poly-silazane precursors, used for the production of silicon oxycarbide (SiOC) and silicon carbonitride (SiCN) ceramics respectively, have significant potential for the fabrication of advanced components. Preceramic polymer derived SiOC foams have been manufactured by following many different processing strategies [3,10–13]. Among these routes, foaming has been achieved by using

* Corresponding author at: Dipartimento di Ingegneria Meccanica-Settore Materiali, Università di Padova Via Marzolo, 9. 35131 Padova, Italy.
Tel.: +39 049 8275825; fax: +39 049 8275505.
E-mail address: paolo.colombo@unipd.it (P. Colombo).

sacrificial processing aids such as polyurethane (PU) [2,10,14,15], poly(methylmetacrylate) (PMMA) microbeads [1,3,5,11,16–18] and foaming agents such as azodicarbonic acid diamide (ADA) [19]. Each of these decomposing agents has its own benefits and drawbacks as regards to manufacturing. The use of sacrificial microspheres has been shown to give better microstructural control (homogeneous pore distribution) on the resulting ceramic foam. Particularly, it was shown that foams produced with PMMA microbeads [17] display better mechanical properties than those of macro-cellular foams of the same density, because of smaller struts (hence smaller critical flaws) and the presence of a smaller amount of processing defects (micro-cracks) in micro-cellular ceramics. It should be noted that the low mechanical properties of ceramic foams produced by using ADA were attributed both to the inhomogeneity of the microstructure and the defects therein [19]. Direct blowing of pure polysiloxanes, without any aid of other additives, has also been employed to fabricate SiOC macro-cellular foams [20,21] and micro-cellular foams [22], while supercritical CO_2 enabled to obtain micro-cellular foams [12].

Although foaming in SiOC system has been intensively studied in the past, only few papers have been published so far concerning highly porous SiCN ceramics. It is already known that non-oxide SiCN ceramics have higher chemical, thermal (roughly speaking, onset of T_g for SiOC is 1300 °C [23] and for SiCN is 1400 °C [24]) and microstructural (higher crystallization temperature [25] and higher temperature of carbothermal decomposition) stability in comparison to SiOC ceramics. Moreover, SiCN ceramics possess additional properties such as tailorable electro-magnetic behavior [26–28], luminescence [29,30], high temperature oxidation and creep resistance [31] which make the manufacture of cellular SiCN ceramics of interest in particular for advanced filtering and sorption applications.

Recently, highly porous ceramic monoliths possessing pore diameters ranging from 50 nm to 10 μm were obtained by the pyrolysis of polysilazane-filled packed beds of polystyrene (PS) or silica (SiO_2) spheres [32]. Wang et al. [33] manufactured porous SiCN ceramic having 455 m^2/g specific surface area (SSA), with a cell (macropore) size of about 0.1–0.6 μm, by templating the polysilazane precursor with colloidal SiO_2 particles. Likewise, Song et al. [34] produced two-dimensional (2D) ordered macroporous SiCN ceramics by solution dipping method based on the 2D SiO_2 monolayers. However, the removal of hard templates such as silica can damage or contaminate the resulting material [35]. As an alternative to SiO_2 etching, Yan et al. [35] used PS spheres and obtained the SiCN foams with a cell size of 0.5–1 μm, having a SSA of 184.5 and 71 m^2/g, respectively. The authors claimed that the foams produced by PS templating have higher thermal stability comparing with that of those produced by SiO_2 particles due to the lack of damages created during acid etching [35]. Very recently nano-porous PE was used as a template for the synthesis of SiCN ceramic monolith with bicontinuous pore structure having 60–100 nm pores [36]. However, none of these studies reported any data concerning the mechanical properties

of the SiCN foams produced, and the above processing procedures are more suitable to the production of components with small dimensions, because of the difficulty in packing very small beads on a large, three-dimensional scale. Moreover, large cell sizes (e.g., in the range 10–1000 μm) were never obtained.

The aim of the present study was to produce highly porous micro- and macro-cellular SiCN foams possessing interconnected cells with a dimension ranging from a few microns to a few hundred microns. Two different processing routes were employed: (I) templating with sacrificial polymeric beads, and (II) direct blowing using a physical blowing agent.

2. Experimental procedure

Ceramic foams were produced by using a commercially available poly(methylvinyl)silazane (Ceraset^{TM} VL20, KiON Corporation, Clariant, USA), as SiCN precursor, mixed, in partially cross-linked state, with poly(methylmetacrylate) (PMMA) microbeads of 20 μm nominal size (Aldrich Chemical Company Inc., USA), acting as sacrificial filler, and, as received, with azodicarbonamide (ADA, Sigma–Aldrich, USA) as physical blowing agent.

Different processing routes were followed to prepare the green bodies. In processing route I (PMMA sacrificial microbeads), liquid polysilazane was first partially cross-linked by heating in a vertical tube furnace under Ar flow with heating rate of 1 °C/min up to 300 °C (dwelling time 8 h). The heating schedule was chosen in order to achieve a suitable compromise between the polymer meltability, required during the warm pressing step, and its capability of retaining the original shape, necessary during the sacrificial filler burn-out. The pre-crosslinked polymer (abbreviated as PCVL20 in the following) was ground in a planetary ball mill at 180 rpm for 2 h, followed by sieving. The pre-crosslinked precursor powder was dry mixed with PMMA microbeads in two different PCVL20/PMMA weight ratios, 20/80 and 30/70. The powders were homogenized by planetary ball-milling at 180 rpm for 2 h, and the mixture was then warm pressed in air for 2 h at 165 °C (the actual temperature inside the mold was measured by a calibrated K type thermocouple) in a metallic die with a uniaxial hydraulic press equipped with heating plates (warm press Type 123, Collin Technology, Aichach, Germany), by applying a pressure of 13 MPa. Prior to each pressing, the rectangular mold (40 mm × 30 mm) was sprayed with silicone oil to reduce the friction between the green body and the pressing form. The green bodies were subsequently pyrolyzed in a quartz tube furnace (Gero, Germany) in the presence of flowing Ar (99.999% pure). Samples were heated to 450 °C with a rate of 0.5 °C/min, held for 3 h in order to guarantee the complete decomposition of the sacrificial beads, and then pyrolyzed at 1100 °C (heating rate 2 °C/min) for 2 h, followed by cooling in the furnace.

In processing route II (physical blowing agent), ADA powder was mixed with liquid polysilazane under Ar atmosphere, using standard Schlenk techniques. ADA was added to the liquid precursor at concentrations of 1, 3 and 6 wt% under

Table 1
Sample labels and composition (wt%).

Sample	Polysilazane (VL20)	PMMA	ADA
P-SiCN-1	30 (Pre-cured)	70	0
P-SiCN-2	20 (Pre-cured)	80	0
A-SiCN-1	99	0	1
A-SiCN-2	97	0	3
A-SiCN-3	94	0	6

magnetic stirring at room temperature. The homogenous mixtures, after 12 h of stirring, were poured separately in aluminum trays and cured at 300 °C for 4 h (with 2 °C/min heating and cooling rate) under N$_2$ atmosphere (99.999% pure). During this treatment curing and blowing was accomplished (ADA decomposes completely in the 200–300 °C range, see later), and the foamed polymer monoliths were then pyrolyzed under nitrogen at 1100 °C for 2 h (2 °C/min heating and cooling rate) in an alumina tube furnace. In Table 1 the compositions of the prepared samples, using either processing procedure I or II, are reported.

TGA–DTA measurements were carried out with a 2 °C/min heating rate up to 1200 °C under Ar (Netzsch STA 429, Selb, Germany) for the samples prepared with PMMA, and under N$_2$ for the samples obtained using the blowing agent. The true density was measured from finely ground ceramic powder using a He-Pycnometer (Pycnomatic ATC, Porotec). Bulk densities, open and closed porosity of the sintered ceramics were determined by the Archimedes principle (ASTM C373-72), using xylene as buoyant medium.

The crushing strength of the foams was measured at room temperature by compression, using (Instron 5569 UTM, Norwood, MA, USA; cross-head speed of 0.5 mm/min), on samples of nominal size ~5 mm × 5 mm × 10 mm, cut from larger specimens. Each data point represents the average value of five to ten individual tests. The C, N and O content of the ceramics were analyzed by hot gas extraction using a C-Analyzer Leco C-200 and NO-Analyzer Leco TC-436, respectively (LECO Instrument GmbH, Mönchengladbach, Germany). The morphological features of the PDC foams were analyzed from fresh fracture surfaces using a scanning electron microscope (JSM-6300F SEM, JEOL, Tokyo, Japan). SEM images were subsequently analyzed with the ImageTool software (UTHSCSA, University of Texas, USA) to quantify the cell size and cell size distribution. The raw data obtained by image analysis were converted to 3D values to obtain the effective cell dimension through the well-known stereological equation: $D_{sphere} = D_{circle}/0.785$ [37].

3. Results and discussion

Ceramics in the Si–C–N ternary system are usually obtained by the pyrolysis of poly(silazane) polymers. These precursors are characterized by repeating units of silicon and nitrogen atoms in their backbone, and one of the most popular commercial precursor in this category is polyurea(methylvinyl)silazane (PUMVS) of Kion Corporation (Ceraset^{TM}). The only difference between the specific polysilazane precursor used in this study (Ceraset^{TM} VL20), and PUMVS (Ceraset^{TM}), is that the latter contains urea functionality and more low molecular weight silazane components [38]. Therefore, the literature data regarding PUMVS could be used as a reference for comparison purposes.

PUMVS cures thermally between 250 and 480 °C in inert atmosphere, by hydrosilylation and addition of vinyl groups, without the need of any peroxide radical initiator and catalyst [39]. The ceramization of the polymer takes place predominately between 500 and 800 °C. Thermolysis at 1100 °C in inert atmosphere results in an amorphous material with ceramic yield of 70–80% [39]. Further increases in temperature induce the crystallization of nano-sized silicon carbide and silicon nitride [40]. Rigorously speaking, it was shown that amorphous SiCN ceramic derived from PUMVS at 1100 °C is located in the Si$_3$N$_4$, SiC and carbon tri-phase equilibrium area ($p = 1$ Bar N$_2$) and is stable up to 1440 °C [39], when the carbothermal reduction of Si$_3$N$_4$ starts to form SiC [41]. X-ray diffraction analysis (not reported here for the sake of brevity) confirmed that both the micro- and macro-cellular ceramics obtained by pyrolysis at 1100 °C were X-ray amorphous.

3.1. Micro-cellular foams (sacrificial microbeads fillers)

A schematic overview of the process is reported in Fig. 1.
The following key points should be emphasized: (I) the viscosity of the preceramic polymer has to be kept sufficiently low to ensure that the sacrificial beads will be covered completely and homogenously during the warm pressing step; (II) the polymer should be able to retain the shape and the integrity of the morphology in order to avoid collapsing during the template burn-out in pyrolysis; (III) the polymer should not be excessively pre-crosslinked, in order to avoid cracking during the PMMA burn-out. Depending on the characteristics of the preceramic polymer (directly related to its synthesis process), the forming step can significantly vary; for instance the mixture of the preceramic polymer and template can be compacted by either warm [16,17] or cold pressing [1,11]. For warm pressing, besides the degree of cross-linking of the precursor, processing parameters such as forming time, temperature and pressure are very important. Pressing at 165 °C for 60 min of the pre-crosslinked powders yielded flawless samples before and after pyrolysis (see Fig. 2a–c).

As it can be seen from Fig. 3, the main decomposition step of pure precured VL20 occurs between 400 and 800 °C, corresponding to a weight loss of 19%. These data are in accordance with those reported by Li et al. [39] for PUMVS, and are directly related to the initial degree of cross-linking of the preceramic polymer. The degradation of the pure PMMA beads starts at 220 °C and completes at around 420 °C. The TGA curve of sample P-SiCN-1 shows a shift of the decomposition to lower temperatures in comparison to that of pure PMMA, while for sample P-SiCN-2 the degradation starts at higher temperatures. Since it is not possible to extrapolate a linear behavior in accordance with the rule of mixtures, it can be inferred that the PMMA beads and the

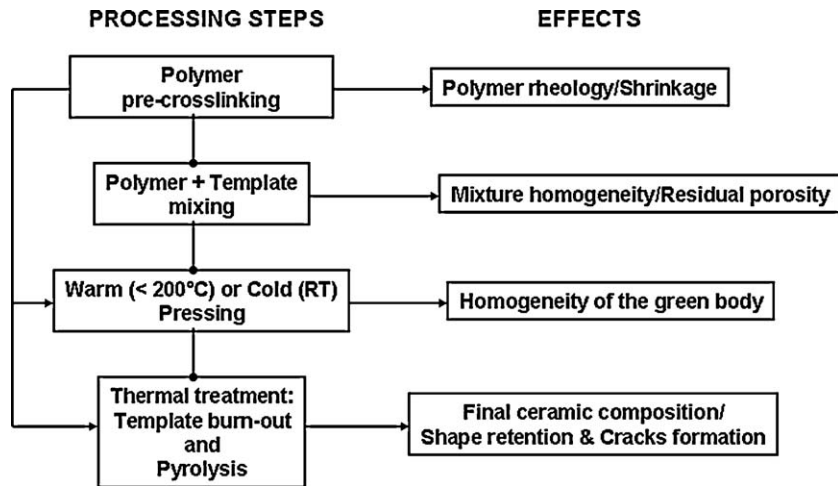**PROCESSING STEPS** | **EFFECTS**

Fig. 1. A schematic overview of the process employing sacrificial templates. The dot connectors refer to the sequence of the process, while arrow connectors highlight the effects of each step on subsequent processing stages and on the characteristics of the final component.
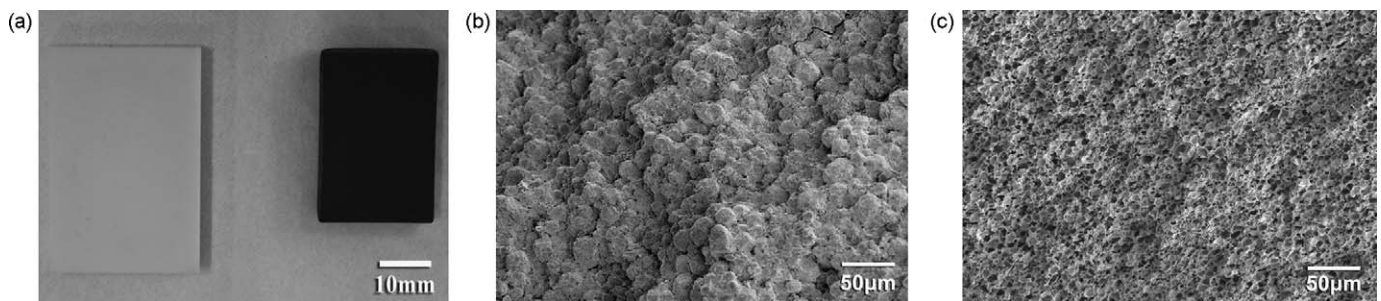

Fig. 2. Sample P-SiCN-2 (80/20): (a) after warm pressing (left) and pyrolysis (right); (b) after warm pressing (165 °C, 1 h); and (c) after pyrolysis (1100 °C, 2 h).

cross-linked silicon polymer have a mutual influence on their thermal stability. After the complete decomposition of PMMA at $T > 400$ °C, the further mass loss is due to the degradation of the PCVL20 fraction, exclusively. This finding is in accordance with the TGA of the pure PCVL20. A slow heating rate (1 °C/min) and a dwelling time of 3 h at 450 °C were

Fig. 3. TGA analysis (Ar) of PCVL20, PMMA microbeads and samples P-SiCN-1 (30/70) and P-SiCN-2 (20/80).

therefore chosen in order to burn-out the PMMA beads and at the same time allowing the pyrolysis gases to escape through the interconnected porosity without causing cracking. Between 800 and 1200 °C the weight loss of PCVL20 was almost negligible, indicating the complete ceramization of the preceramic precursor.

The measured total mass loss data for samples P-SiCN-1 (30/70) and P-SiCN-2 (20/80) at 1100 °C were 73.8% and 82.3%, respectively. These values are comparable with the theoretical calculation data (considering a ceramic yield of 81% for the PCVL20) namely; 75.7% and 83.8%. The mass loss difference could be attributed to the presence of oxygen in the final ceramic. In fact, elemental analysis (EA) revealed that the amount of oxygen in sample P-SiCN-2 (20/80) was 24 wt%, and it was 33 wt% in sample P-SiCN-1 (30/70) (see Table 2). Cross et al. [42] recently reported that the amount of C, O and N in the $SiO_xC_yN_z$ system has a profound effect on the tribological properties of resulted ceramic. Nevertheless, none of the studies mentioned before concerning the SiCN ceramic foams had given information about the final chemical composition. Although highly depending on the processing method employed, it is known that SiCN ceramics produced from preceramic polymers often contain significant amounts of oxygen, due to the high sensitivity of the precursor polymer to moisture [42]. For example, it was shown that the oxygen level could be kept under 1 wt% [39] or could be as high as 27 wt%
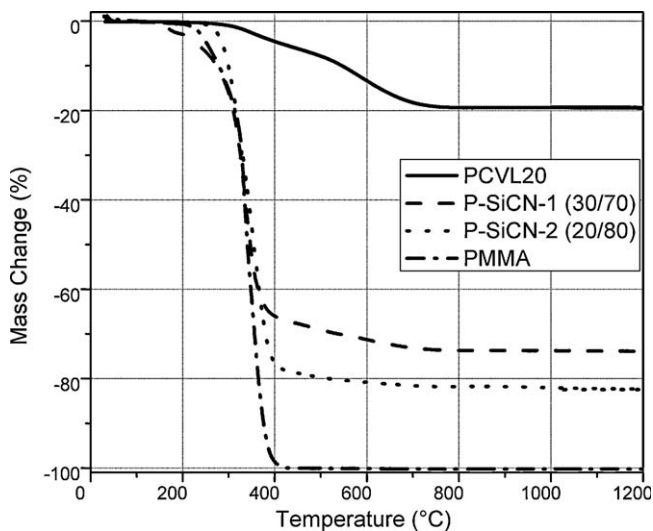
Table 2
Density, porosity, compression strength and approximate empirical formula of Si(O)CN foams produced using sacrificial fillers along with the standard deviation values.

Sample	ρ_{bulk} (g/cm^{-3})	Relative density	P_{total} (vol%)	P_{open} (vol%)	P_{closed} (vol%)	σ (MPa)	SiO$_x$C$_y$N$_z$
P-SiCN-1 (30/70)	0.885 ± 0.01	0.387 ± 0.01	61.1 ± 1.38	50.0 ± 1.07	11.1 ± 0.29	11.6 ± 1.1	SiO$_{1.61}$C$_{1.85}$N$_{0.17}$
P-SiCN-2 (20/80)	0.520 ± 0.01	0.227 ± 0.01	77.24 ± 0.57	73.94 ± 1.28	3.3 ± 0.71	5.6 ± 0.7	SiO$_{0.78}$C$_{0.59}$N$_{0.36}$

[42], for coupons of PUMVS precursor pyrolyzed at 1000 °C in N$_2$ overpressure. The oxygen intake, in the present study, could be attributed to the combined effects of (a) accumulation of oxygen due to the evaporation of volatile C containing components [43], (b) presence of residual humidity on the PMMA beads, and (c) relatively high sensitivity of the preceramic polymer to moisture (during ball milling and warm pressing) [42], and (d) presence of silicone oil used for the lubrication of the mold.

The bulk density and the total and open porosity values are reported in Table 2, including the data from compression tests measurements.

It is not easy to speculate on these results since the mechanical properties of cellular SiCN ceramics have not been yet covered in the literature. The model proposed by Gibson and Ashby for brittle materials [44] could be applicable only to the sample made by using 80 wt% of PMMA microbeads, since the relative density for the sample made by using 70 wt% PMMA was higher than 0.3, for which the validity of the model is exceeded. Therefore, sample SiCN-1 (70/30) should be considered to be a highly porous component rather than a true foam. In Gibson and Ashby's micromechanical bending model for cellular materials, the morphology of closed-cell foams is considered one in which the cell walls are completely retained and do not contain any openings (cell windows). In the same model, the morphology of open-cell foams is idealized as interconnected ligaments without any cell walls (typical microstructure of "reticulated foams" produced by the replica method). Even if the samples prepared by sacrificial templating in the present study can be considered as open cell foams due to their mostly interconnected porosity, the morphology of the foams, as shown in Fig. 4a and b, is much more similar to that of the closed foams in which the cell walls are mostly retained. Therefore, it is reasonable that the strength data for our samples

are more descriptive to what the model predicts for closed-cell foams. Similar behavior was previously observed by Colombo et al. [2] for SiOC foams. Due to the limited amount of data available, it was not possible to ascertain the value for the exponent for the logarithmic correlation function linking relative density and relative strength [3,44]. However, the increase in compression strength values with the increase of bulk density is here confirmed, and the strength values measured were rather high, and comparable to what observed for SiOC micro-cellular foams [11].

SEM micrographs (Fig. 4a and b) show that a great amount of porosity, mostly interconnected, was formed in both samples, with pores ranging from about 5 μm to 15 μm in size. Roughly spherical shaped cells were homogeneously distributed throughout the entire volume of the pyrolyzed ceramic monoliths. Cell size and shape were not precisely similar to those of the PMMA templating beads, because of the large amount of volumetric shrinkage occurring during the ceramization step (~70 vol%). However, the distribution in cell sizes resembles that of the original PMMA microbeads.

The amount of the total porosity increased with the increased amount of sacrificial templates, while closed porosity showed the opposite trend. It should be noticed that a small amount of porosity may be attributed to other factors than the presence of the sacrificial microbeads. In fact, it was reported that warm pressed pre-crosslinked polysilazane powders possessed ~3 vol% porosity after pyrolysis at 1100 °C [45]. The increased amount of closed porosity in samples SiCN-1 (70/30) could be attributed to the higher amount of preceramic polymer in the starting mixture and to the lower amount of PMMA beads that could cause a partial non-contact among the same beads, consequently giving rise to thicker struts and cell walls.
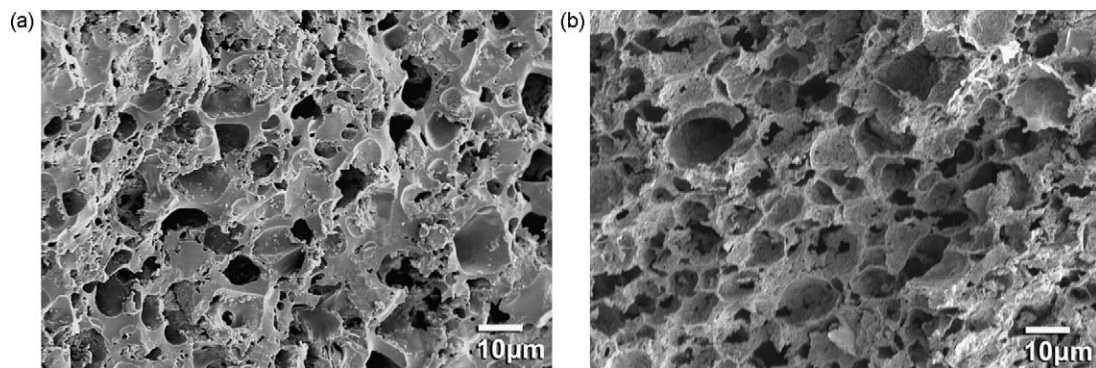

Fig. 4. SEM micrographs of the fracture surface of pyrolyzed samples: (a) SiCN-1 (70/30) and (b) P-SiCN-2 (80/20).

3.2. Macro-cellular foams (physical blowing agent)

For in-situ foaming with a physical blowing agent, ADA was selected since its gas yield during decomposition is very high (200–220 mL/g), which makes it the most cost efficient among all commercially available foaming agents [46]. In order to examine the effects of the porogen amount on the morphology and other characteristics, ADA was inserted into the liquid polysilazane precursor in increasing amounts (see Table 1). The decomposition onset temperature for pure ADA is around 210 °C [19], and the gas released consists mostly of nitrogen (65 vol%) and a mixture of carbon monoxide, carbon dioxide, and ammonia [19,47]. The solid residue after decomposition consists of urazol, biurea, cyamelide, and cyanuric acid [48]. Depending on the processing conditions, different compositions in the end-product may be favored; however it was shown that there is always some amount of solid residue acting as a nucleating agent for the blowing process during decomposition. The decomposition reaction was found to be autocatalytic, resulting in a color change from yellow to a more neutral one [49,50].

In the literature, many studies can be found concerning foaming of various polymeric systems using ADA [19,47,49,51]. In situ foaming with porogens necessitates a good control between the activation (rate, temperature) of the blowing agent and the melt viscosity of the precursor polymer. If the blowing agent decomposes before the polymeric precursor possesses sufficient enough melt viscosity to maintain the gas within the matrix, there will not be foaming. On the contrary, the polymer viscosity could be too high during the decomposition of the porogen so that insufficient gas pressure cannot initiate blowing, even though decomposition has occurred. For that reason, various parameters such as the decomposition temperature and rate of the blowing agent and the processing conditions of the precursor matrix must all be considered before a polymeric

material is selected [46]. Moreover, the decomposition process of porogens can be controlled by varying its particle size, heating rate and processing temperature, activator type and concentration, etc. [46,49] Commonly, some transition metal compounds, polyols, urea, alcohol, amines, and some organic acids such as stearic acid [49] are used as activators to reduce the already mentioned decomposition temperature of ADA to values as low as 150 °C [46].

As one can see from Fig. 5a, the thermo-gravimetric curve of pure ADA used in these experiments showed a decomposition onset at around 210 °C, and off-set at around 320 °C, with a large weight loss reaching 88 wt%; a clear exothermic peak can be observed at 210 °C (Fig. 5b). The solid residue contamination as a result of ADA decomposition within the foamed ceramic was therefore very limited (≤1.1 wt%).

At 300 °C, the mass loss for pure VL20 was around 10 wt%, and around 20 wt% for the samples containing ADA. The increased mass loss values for the porogen including samples are certainly attributable to the presence of ADA. It appeared that increasing the amount of ADA in the ADA-containing samples decreased the mass loss during the second stage of curing (300–500 °C); all the foamed samples displayed the same behavior during ceramization (in the 500–800 °C range) and no further significant mass loss was detectable between 800 and 1200 °C. However, unexpectedly, at the end of the pyrolysis the measured ceramic yield was lower than the one computed on the basis of the rule of mixture (theoretical) especially for the samples fabricated from 1 and 3 wt% of ADA. The effect attributable to the higher mass losses (compared to theoretical calculations) for the ADA including samples could arise due to enhanced release of gaseous by-products due both to the curing reactions and especially to the evaporation of low molecular weight components (Si-containing oligomers) occurring before such reactions link all the polymeric chains into a three-dimensional network.
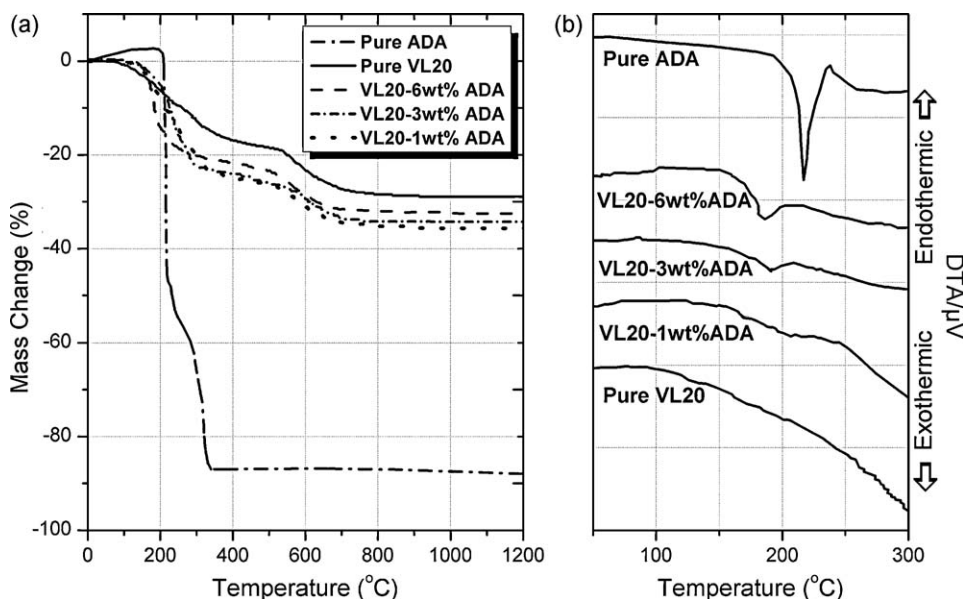

Fig. 5. TG/DTA results for pure ADA, pure VL20 and all other samples made by using VL20 and ADA (under N_2 flow).

For the samples made by using ADA there was an increase in the ceramic yield (lower total weight loss) with increasing incorporation of ADA. This implies that there was an interaction between VL20 and ADA which presumably altered the branching or cross-linking sequence of the polymer depending on the amount of ADA. The use of peroxide or azo compounds as free radical initiators is indeed recommended to promote vinyl crosslinking of silazane precursor [38]. These groups may facilitate curing when energy is provided even at relatively low temperatures. The exothermic reaction with free radicals decreases the cross-linking temperature and increases the degree of polymer cross-linking. This results in the reduction of evaporable oligomers and an increase of the ceramic yield. For example, the addition of dicumyl peroxide to PUVMS or VL20 leads to a decrease of the cross-linking temperature from 180–250 to 90–190 °C [39]. Furthermore, the degree of transamination might be reduced by the increase in ADA amount. Transamination is also important because it involves cleavage of Si–N bonds, and this may cause the formation of oligomeric units from the cross-linked polymer network [39]. Results from the elemental analyses agreed with the above observation; the increase in the ADA amount led to higher nitrogen content in final ceramics. More specific investigations (e.g., solid state NMR analysis) will have to be performed to ascertain the mechanism leading to an increased ceramic yield with increasing incorporation of ADA in the foamed samples, but this is beyond the scope of the present work. Another possibility is that the interaction between VL20 and ADA activated ADA so that it decomposed at lower temperature than expected (note that the decrease in the particle size of ADA while dispersing in liquid precursor has a parallel effect). In fact, the occurrence of the latter is very clear from the shift to lower temperatures of the exothermic peak linked to ADA decomposition (see Fig. 5b). The sample with 6 wt% ADA showed an exothermic effect around 170 °C, temperature lower than the actual decomposition temperature of pure ADA.

Li et al. [39] have shown that PUMVS can be thermally set into a solid product without any catalyst, and that the transformation from liquid to a solid product is completed in 35 min at 150 °C and in less than 5 min at 280 °C. The authors explained that below 250 °C, the viscosity of the liquid precursor increases to form a gel-like product, and a stable solid can be obtained at 300 °C with a high cross-linking yield.

Likewise, Lücke et al. [52] have demonstrated that after passing a minimum around 120 °C, the melt viscosity values increased rapidly due to hydrosilylation reactions and above 200 °C synthesized poly(methylvinylsilazane) precursor became solid-like. At temperatures higher than 250 °C hydrosilylation reactions came to an end [52], and thereafter vinyl polymerization occurred to form a thermoset [39]. In the present paper, considering the literature data and with reference to TGA results, the curing schedule was selected. Specifically, heating to 300 °C with a 2 °C/min heating rate was found optimal for the sample with 1 wt% of ADA (A-SiCN-1), enabling the complete decomposition of the porogen, while at the same time the melt viscosity of the precursor was suitable to retain the morphological integrity. A further indication for the complete decomposition of ADA could be found from the final color of the thermoset; the yellowish color of the blend turned to an opaque material after processing at 300 °C. Holding at this temperature for 4 h resulted in a foamed polymeric thermoset (see Fig. 6a).

SEM investigations revealed that the samples possessed a regular morphology comprised of homogenously distributed spheroidal cells with a diameter up to 1.5 mm, with circular interconnecting windows having 100–300 μm diameter, and dense struts. Quite a few number of these cell windows were closed by a very thin layer of precursor material (see white arrows). There were no observable cracks in the polymeric cellular matrix. The microstructure of the pyrolyzed monolith, Fig. 6b, closely resembled the one for the thermoset, except that most of the cell windows were open and the cell size was smaller, due to the shrinkage occurring during ceramization (average cell size 735 ± 225 μm). The shrinkage did not cause crack formation, and monoliths having dense struts and homogenously distributed interconnected cells were obtained (see Fig. 6c).

The samples with 3 wt % ADA (images not shown here for brevity) and more evidently the one with 6 wt% ADA contained a gradient in porosity (see Fig. 7a–c). SiOC foams with graded porosity were obtained by other researchers using direct blowing [21,53]. It should be noted that, in general, inclusion of porogens lowers the melt viscosity due to a plasticizing effect of the microbubbles [54]. For instance, the reduction in the melt viscosity of the PE/ADA system was found to be dependent on the concentration of ADA and increasing the amount of ADA decreased the viscosity, due to enhanced plasticizing effect
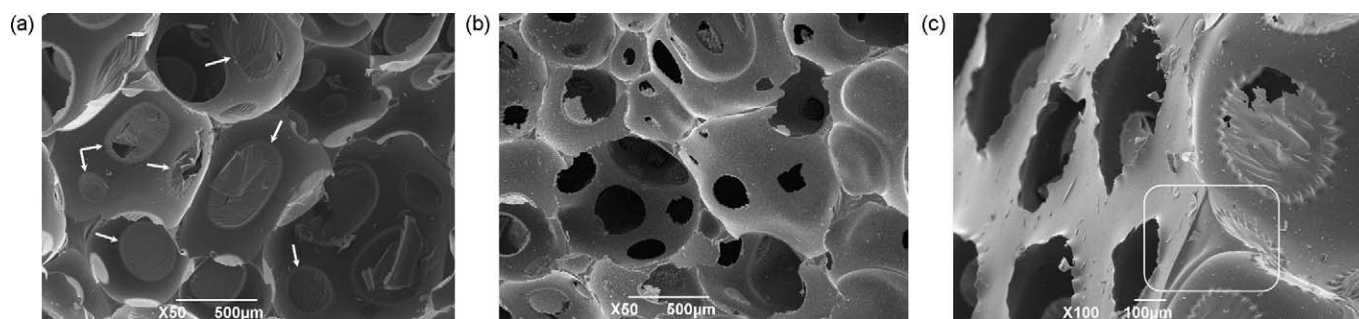

Fig. 6. SEM micrographs of the fracture surface of sample A-SiCN-1: (a) foamed thermostet (at 300 °C; white arrows indicate membranes on cell windows); (b) pyrolyzed monolith (at 1100 °C); and (c) detailed view of pyrolyzed monolith from the edge (white rectangle indicates a representative dense strut).
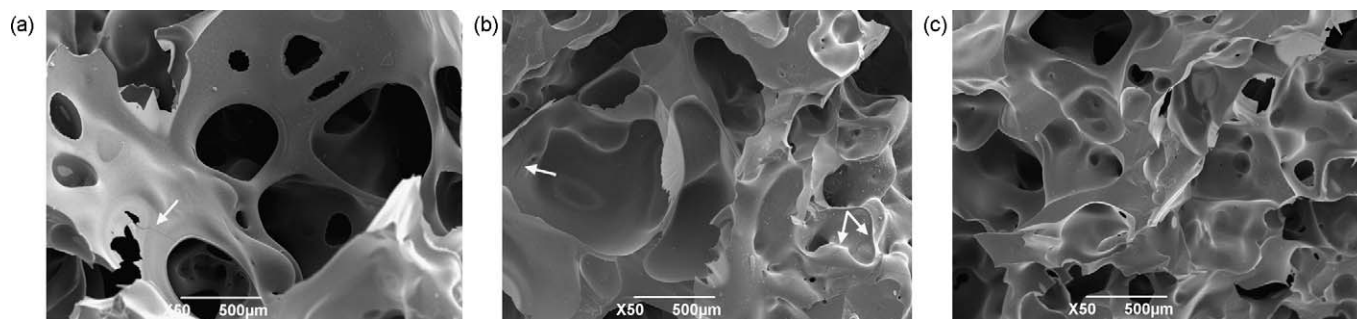
Fig. 7. SEM micrographs of the fracture surface of sample A-SiCN-3 (6 wt% ADA) after pyrolysis at 1100 °C, (a) taken from the bottom; (b) taken from the middle (white arrows indicate cracks); (c) taken from the top.

[54]. These findings suggest that the amount of ADA incorporation in our experiments affected the melt viscosity of the preceramic polymer, and therefore the pore morphology and porosity distribution within the component.

The influence of the melt viscosity of the precursor on the foam morphology was not intentionally investigated here, since it was beyond the scope of the present work, but the study of Takahashi and Colombo [19] on SiOC foams showed that there is a relation between the morphology of a foam produced by direct blowing of a preceramic polymer, and the melt viscosity. Zeschky et al. [21] linked the formation of graded porosity related to a non-linear increase in viscosity, and showed that bubbles three times larger formed at the bottom of the sample compared to the ones at the top. The same behavior was observed in the present study for the samples containing 3 wt % ADA and more visibly 6 wt% ADA (see Fig. 7a–c). In fact, an increased amount of ADA particles enhanced the microbubble nucleation during its decomposition, so that the melt viscosity of the mix decreased due to a plasticizing effect. At this stage, the bubble rise occurred easily, due to low viscosity or the polymer, leading to an accumulation of pores at the foam surface. Continuation of heating yielded a pronounced increase of viscosity due to concurrent curing reactions taking place during bubble formation and bubble rise, analogous to the observations of Zeschky et al. [21]. Moreover, it should be noted that the decomposition of ADA is exothermic. Most probably, homogenously distributed ADA particles acted also as a heat source and locally enhanced the curing reactions. When the viscosity reached a certain minimum level, the ratio of bubble rise velocity to bubble growth rate became less than unity. Hence, the bubbles still could grow at the bottom of the sample due to Ostwald ripening arising from interbubble gas diffusion [20]. Coalescence by film (cell wall) rupture was not observed at that stage, due to the thickness of the lamella and

high viscosity of the polymer (preventing liquid drainage), therefore resulting in smaller cells at the top (<500 μm, see Fig. 7c) and bigger cells at the bottom of the sample (>1 mm, see Fig. 7a). Further increase in viscosity reduced the molecular gas diffusion through the system, thus preventing the possibility of further coarsening and finally yielding a thermoset containing graded porosity along the expansion axis. The produced ceramics with graded pores exhibited differences in structure; while the one with 3 wt% ADA was flawless, the one with 6 wt% ADA had some internal micron-sized cracks (see white arrows in Fig. 7a and b).

All the samples possessed a large amount of porosity after pyrolysis, which was mostly open. Increasing the amount of ADA in the blends led to an increase in the cell size and affected the pore morphology, interconnectivity and amount of porosity. The presence of cells with a non-homogeneous size distribution does not particularly represent a problem since several important properties are not linked to the cell size but rather to the relative density of the component [44]. Correspondingly, in this study the compression strength was found to be dependent on relative density and to the presence of internal defects. The mechanical properties and porosity values of the samples are reported in Table 3. They are lower than the values obtained for micro-cellular SiOCN foams, in accordance with what already observed for SiOC samples [11].

The level of oxygen contamination was found to be very limited when ADA was used as a physical blowing agent. For instance the concentration of oxygen impurity was 0.87 wt% for the sample made by using 1 wt% ADA. This is a very low value and almost the same as that of the ceramic made by using pure VL20 precursor (0.60 wt% of oxygen with an approximate empirical formula of $SiO_{0.02}C_{0.66}N_{0.58}$). The results given in Table 3 indicated that even with the highest amount of ADA

Table 3
Density, porosity, compression strength and approximate empirical formula of SiCN foams produced using a physical blowing agent along with the standard deviation values.

Sample	ρ_{bulk} (g/cm^{-3})	Relative density	P_{total} (vol%)	P_{open} (vol%)	P_{closed} (vol%)	σ (MPa)	$SiO_xC_yN_z$
A-SiCN-1 (1 wt% ADA)	0.687 ± 0.18	0.293 ± 0.08	70.68 ± 8.07	49.45 ± 10.91	21.22 ± 9.74	2.89 ± 1.04	$SiO_{0.03}C_{0.66}N_{0.60}$
A-SiCN-2 (3 wt% ADA)	0.811 ± 0.09	0.344 ± 0.04	64.74 ± 3.90	45.58 ± 5.29	20.16 ± 5.04	3.31 ± 1.38	$SiO_{0.10}C_{0.66}N_{0.70}$
A-SiCN-3 (6 wt% ADA)	0.830 ± 0.21	0.352 ± 0.09	63.92 ± 9.32	47.14 ± 9.02	16.78 ± 8.97	1.08 ± 0.56	$SiO_{0.10}C_{0.66}N_{0.74}$

usage, ceramic foams with substantially low amount of oxygen contamination (<3.32 wt%) could be obtained by the method described in the present study.

4. Conclusions

Two different processing routes have been proposed to fabricate SiCN and SiOCN ceramic foams from a polysilazane preceramic polymer. Pyrolysis of the warm pressed mixture of partially cross-linked polysilazane and PMMA microspheres resulted in microcellular SiOCN ceramics having cell size up to 15 μm. Pre-curing of silazane precursor, PMMA/silazane ratio and warm pressing parameters were found to be important factors in determining the amount of porosity, pore morphology and the degree of interconnections of the cells. In the second route, liquid polysilazane was mixed with a physical blowing agent and the blend was cured and pyrolyzed, leading to the formation of macro-cellular ceramics with ∼70 vol% porosity in a one-step process. With a low amount of blowing agent addition (1 wt%) ceramic foams with regular morphology comprised of homogenously distributed spheroidal cells with a diameter ∼700 μm were produced. Increasing the amount of blowing agent in the precursor led to a porous component with graded porosity with small cells at the top (<500 μm) and large cells at the bottom of the sample (>1 mm). The oxygen contamination in the pyrolyzed ceramic was very limited. The compression strength of macro-cellular foams was lower than those of the micro-cellular samples. It was shown that the polymer derived ceramic (PDC) route is an efficient and versatile way to produce Si(O)CN foams possessing tailored pore architecture and properties suitable for high temperature applications.

Acknowledgments

References

[1] P. Colombo, E. Bernardo, L. Biasetto, Novel microcellular ceramics from a silicone resin, Journal of the American Ceramic Society 87 (1) (2004) 152–154.

[2] P. Colombo, J.R. Hellmann, D.L. Shelleman, Mechanical properties of silicon oxycarbide ceramic foams, Journal of the American Ceramic Society 84 (10) (2001) 2245–2251.

[3] P. Colombo, Engineering porosity in polymer-derived ceramics, Journal of the European Ceramic Society 28 (7) (2008) 1389–1395.

[4] R. Zhuo, P. Colombo, C. Pantano, E.A. Vogler, Silicon oxycarbide glasses for blood-contact applications, Acta Biomaterialia 1 (5) (2005) 583–589.

[5] L. Biasetto, A. Francis, P. Palade, G. Principi, P. Colombo, Polymer-derived microcellular SiOC foams with magnetic functionality, Journal of Materials Science 43 (12) (2008) 4119–4126.

[6] P. Colombo, T. Gambaryan-Roisman, M. Scheffler, P. Buhler, P. Greil, Conductive ceramic foams from preceramic polymers, Journal of the American Ceramic Society 84 (10) (2001) 2265–2268.

[7] P. Colombo, J.R. Hellmann, D.L. Shelleman, Thermal shock behavior of silicon oxycarbide foams, Journal of the American Ceramic Society 85 (9) (2002) 2306–2312.

[8] P. Colombo, Conventional and novel processing methods for cellular ceramics, Philosophical Transactions of the Royal Society A: Mathematical, Physical and Engineering Sciences 364 (1838) (2006) 109–124.

[9] P. Colombo, M. Scheffler, Highly porous components, in: P. Colombo, G.D. Sorarù, R. Riedel, A. Kleebe (Eds.), Polymer-derived-ceramics, DESTech Publications, Lancaster, PA, 2009.

[10] P. Colombo, M. Modesti, Silicon oxycarbide ceramic foams from a preceramic polymer, Journal of the American Ceramic Society 82 (3) (1999) 573–578.

[11] P. Colombo, E. Bernardo, Macro- and micro-cellular porous ceramics from preceramic polymers, Composites Science and Technology 63 (16) (2003) 2353–2359.

[12] Y.-W. Kim, C.B. Park, Processing of microcellular preceramics using carbon dioxide, Composites Science and Technology 63 (16) (2003) 2371–2377.

[13] C. Vakifahmetoglu, P. Colombo, A Direct method for the fabrication of macro-porous SiOC ceramics from preceramic polymers, Advanced Engineering Materials 10 (3) (2008) 256–259.

[14] T. Takahashi, H. Münstedt, M. Modesti, P. Colombo, Oxidation resistant ceramic foam from a silicone preceramic polymer/polyurethane blend, Journal of the European Ceramic Society 21 (16) (2001) 2821–2828.

[15] H. Schmidt, D. Koch, G. Grathwohl, P. Colombo, Micro-/macroporous ceramics from preceramic precursors, Journal of the American Ceramic Society 84 (10) (2001) 2252–2255.

[16] S. Costacurta, L. Biasetto, E. Pippel, J. Woltersdorf, P. Colombo, Hierarchical porosity components by infiltration of a ceramic foam, Journal of the American Ceramic Society 90 (7) (2007) 2172–2177.

[17] M. Shibuya, T. Takahashi, K. Koyama, Microcellular ceramics by using silicone preceramic polymer and PMMA polymer sacrificial microbeads, Composites Science and Technology 67 (1) (2007) 119–124.

[18] Y.-W. Kim, S.-H. Kim, H.-D. Kim, C.B. Park, Processing of closed-cell silicon oxycarbide foams from a preceramic polymer, Journal of Materials Science 39 (18) (2004) 5647–5652.

[19] T. Takahashi, P. Colombo, SiOC ceramic foams through melt foaming of a methylsilicone preceramic polymer, Journal of Porous Materials 10 (2003) 113–121.

[20] T. Fujiu, G.L. Messing, W. Huebner, Processing and properties of cellular silica synthesized by foaming sol–gels, Journal of the American Ceramic Society 73 (1) (1990) 85–90.

[21] J. Zeschky, T. Höfner, C. Arnold, R. Weißmann, D. Bahloul-Hourlier, M. Scheffler, P. Greil, Polysilsesquioxane derived ceramic foams with gradient porosity, Acta Materialia 53 (4) (2005) 927–937.

[22] R. Rocha, E. Moura, A. Bressiani, J. Bressiani, SiOC ceramic foams synthesized from electron beam irradiated methylsilicone resin, Journal of Materials Science 43 (13) (2008) 4466–4474.

[23] A. Saha, R. Raj, Crystallization maps for SiCO amorphous ceramics, Journal of the American Ceramic Society 90 (2007) 578–583.

[24] H.J. Seifert, J. Peng, H.L. Lukas, F. Aldinger, Phase equilibria and thermal analysis of Si–C–N ceramics, Journal of Alloys and Compounds 320 (2) (2001) 251–261.

[25] M. Friess, J. Bill, J. Golczewski, A. Zimmermann, F. Aldinger, R. Riedel, R. Raj, Crystallization of polymer-derived silicon carbonitride at 1873 K under nitrogen overpressure, Journal of the American Ceramic Society 85 (10) (2002) 2587–2589.

[26] E. Kroke, Y.-L. Li, C. Konetschny, E. Lecomte, C. Fasel, R. Riedel, Silazane derived ceramics and related materials, Materials Science and Engineering: R: Reports 26 (4–6) (2000) 97–199.

[27] A. Saha, S.R. Shah, R. Raj, S.E. Russek, Polymer-derived SiCN composites with magnetic properties, Journal of Materials Research 18 (11) (2003) 2549–2551.

[28] C. Haluschka, C. Engel, R. Riedel, Silicon carbonitride ceramics derived from polysilazanes. Part II. Investigation of electrical properties, Journal of the European Ceramic Society 20 (9) (2000) 1365–1374.

[29] I. Menapace, G. Mera, R. Riedel, E. Erdem, R.-A. Eichel, A. Pauletti, G. Appleby, Luminescence of heat-treated silicon-based polymers: promising

materials for LED applications, Journal of Materials Science 43 (17) (2008) 5790–5796.

[30] X.-W. Du, Y. Fu, J. Sun, P. Yao, The evolution of microstructure and photoluminescence of SiCN films with annealing temperature, Journal of Applied Physics 99 (9) (2006) 093503–093504.

[31] G. Thurn, J. Canel, J. Bill, F. Aldinger, Compression creep behaviour of precursor-derived Si–C–N ceramics, Journal of the European Ceramic Society 19 (13–14) (1999) 2317–2323.

[32] I.-K. Sung, M.M. Christian, D.-P. Kim, P.J.A. Kenis, Tailored macroporous SiCN and SiC structures for high-temperature fuel reforming, Advanced Functional Materials 15 (8) (2005) 1336–1342.

[33] H. Wang, S.-Y. Zheng, X.-D. Li, D.-P. Kim, Preparation of three-dimensional ordered macroporous SiCN ceramic using sacrificing template method, Microporous and Mesoporous Materials 80 (1–3) (2005) 357–362.

[34] I.-H. Song, Y.-J. Kim, H.-D. Kim, D.-P. Kim, Colloidal crystal templating of two-dimensional ordered macroporous SiCN ceramics, Solid State Phenomena 135 (2008) 27–30.

[35] J. Yan, L.-Y. Hong, A. Wang, D.-P. Kim, Facile synthesis of SiCN ceramic foam via self-sacrificial template method, Solid State Phenomena 124–126 (2007) 727–730.

[36] B.H. Jones, T.P. Lodge, High-temperature nanoporous ceramic monolith prepared from a polymeric bicontinuous microemulsion template, Journal of the American Chemical Society 131 (5) (2009) 1676–1677.

[37] ASTM D 3576, Standard test method for cell size of rigid cellular plastics, in: Annual Book of ASTM Standards, vol. 08.02, West Conshohocken, PA, 1997.

[38] Technical Bulletin 1, KiON Ceraset polyureasilazane and KiON ceraset polysilazane 20 heat-curable resins of KiON Corporation, http://www.kioncorp.com/bulletins.html (Last accessed 03.09).

[39] Y.-L. Li, E. Kroke, R. Riedelm, C. Fasel, C. Gervais, F. Babonneau, Thermal cross-linking and pyrolytic conversion of poly(ureamethylvinyl)silazanes to silicon-based ceramics, Applied Organometallic Chemistry 15 (10) (2001) 820–832.

[40] H. Schmidt, G. Borchardt, A. Müller, J. Bill, Formation kinetics of crystalline Si3N4/SiC composites from amorphous Si–C–N ceramics, Journal of Non-Crystalline Solids 341 (1–3) (2004) 133–140.

[41] D. Seyferth, C. Strohmann, N.R. Dando, A.J. Perrotta, Poly(ureidosilazanes): preceramic polymeric precursors for silicon carbonitride and silicon nitride. Synthesis, characterization, and pyrolytic conversion to Si3N4/SiC ceramics, Chemistry of Materials 7 (11) (1995) 2058–2066.

[42] T. Cross, R. Raj, S.V. Prasad, T.E. Buchheit, D.R. Tallant, Mechanical and tribological behavior of polymer-derived ceramics constituted from $SiC_xO_yN_z$, Journal of the American Ceramic Society 89 (12) (2006) 3706–3714.

[43] S. Gumann, N. Nestle, V. Liebau-Kunzmann, R. Riedel, Investigations of Li-containing SiCN(O) ceramics via 7Li MAS NMR, Solid State Nuclear Magnetic Resonance 31 (2) (2007) 82–90.

[44] L.J. Gibson, M.F. Ashby, Cellular Solids, Structure and Properties, Cambridge University Press, UK, 1999.

[45] C. Konetschny, D. Galusek, S. Reschke, C. Fasel, R. Riedel, Dense silicon carbonitride ceramics by pyrolysis of cross-linked and warm pressed polysilazane powders, Journal of the European Ceramic Society 19 (16) (1999) 2789–2796.

[46] S. Quinn, Chemical blowing agents: providing production, economic and physical improvements to a wide range of polymers, Plastics, Additives and Compounding 3 (2001) 16–21.

[47] A.S.P. Lin, T.H. Barrows, S.H. Cartmell, R.E. Guldberg, Microarchitectural and mechanical characterization of oriented porous polymer scaffolds, Biomaterials 24 (3) (2003) 481–489.

[48] A.S. Prakash, W.A. Swam, A.N. Strachan, The thermal decomposition of azodicarbonamide (1,1-azobisformamide), J. Chem. Soc., Perkin Trans. 2 (1975) 46–50.

[49] J.R. Robledo-Ortiz, C. Zepeda, C. Gomez, D. Rodrigue, R. González-Núñez, Non-isothermal decomposition kinetics of azodicarbonamide in high density polyethylene using a capillary rheometer, Polymer Testing 27 (6) (2008) 730–735.

[50] L. Rychlá, J. Rychlý, J. Svoboda, J. Šimonik, DSC study of the decomposition of azodicarbonamide in different media, Journal of Thermal Analysis and Calorimetry 29 (1) (1984) 77–85.

[51] Q. Huang, R. Klotzer, B. Seibig, D. Paul, Extrusion of microcellular polysulfone using chemical blowing agents, Journal of Applied Polymer Science 69 (9) (1998) 1753–1760.

[52] J. Lücke, J. Hacker, D. Suttor, G. Ziegler, Synthesis and characterization of silazane-based polymers as precursors for ceramic matrix composites, Applied Organometallic Chemistry 11 (2) (1997) 181–194.

[53] P. Colombo, J. Hellmann, Ceramic foams from preceramic polymers, Materials Research Innovations 6 (5) (2002) 260–272.

[54] X. Qin, M.R. Thompson, A.N. Hrymak, A. Torres, Rheology studies of polyethylene/chemical blowing agent solutions within an injection molding machine, Polymer Engineering & Science 45 (8) (2005) 1108–1118.